System Architecture for Low Power Ubiquitously Connected Remote Health Monitoring Applications With Smart Transmission Mechanism

M. P. R. Sai Kiran, Y. Siva Krishna, P. Rajalakshmi, Amit Acharyya,

***Abstract*—We present a novel smart transmission technique with seamless hand-off mechanism to achieve ubiquitous connectivity using multiple on-chip radios targeting remote health monitoring applications. For the first time to the best of our knowledge, a system architecture for low power ubiquitously connected multi parametric remote health monitoring system is discussed in this paper. The architecture proposed uses a generic adaptive rule engine for classifying the collected multi parametric data from patient and smartly transmit the data when only needed. The on-chip seamless hand-off mechanism proposed aids for the ubiquitous connectivity with a very good energy savings by intelligent controlling of the multiple on-chip radios. The performance analysis of the proposed on-chip seamless hand-off mechanism along with adaptive rule engine based smart transmission mechanism achieves on an average of 50.39% of energy saving and 51.01% reduction in duty cycle of transmitter taken over 20 users compared to the continuous transmission. From the hardware complexity analysis made on the proposed seamless hand-off controller and adaptive rule engine shows that they require 2196 CMOS transistors for implementation.**

***Index Terms*—Ubiquitous connectivity, Seamless hand-off, RSSI, path loss model, Random Waypoint Mobility (RWP).**

I. Introduction

IN remote health monitoring the proactive diagnosis is mainly constrained due to the unavailability of the patient under ubiquitous monitoring. The primary reasons for this scenario are the user is non-static (thereby user crosses the range of connectivity) and life time of the node. To address this issue we propose a system architecture for multi parametric remote health monitoring which can be connected ubiquitously and consumes less energy. For achieving ubiquitous connectivity, a seamless hand-off controller is developed which intelligently controls multiple on-chip radios during data transmission. The seamless hand-off controller drastically reduces the energy consumption by efficiently using multiple on-chip radios which have different energy consumptions. In addition to the energy saving achieved by the seamless hand-off controller, a generic adaptive rule engine based smart transmission mechanism is included in the architecture, which classifies the data and transmits only when needed. The adaptive rule engine reduces the data traffic transmitted significantly without any loss of data thereby maintaining reliability.

*This work is partly supported by the DEITY, India under the "IOT for Smarter Healthcare" under Grant No: 13(7)/2012-CC&BT, Dated 25th Feb, 2013.

M.P.R.S.K., Y.S.K., P.R. and A.A. are with Department of Electrical Engineering, Indian Institute of Technology Hyderabad, 502205, India with email {ee12m1021,ee14resch11008,raji,amit_acharyya}@iith.ac.in respectively

Many architectures for remote health monitoring procedures were developed in the recent years such as [1], [2] & [3]. In [1], the remote health monitoring system is based on the smart phone for enabling the real time monitoring and full Internet Protocol (IP) connectivity has been used. The problems that occur due to the improper data association collected from patients have been discussed in [2]. The architecture proposed in [2] consists of a central gateway which gathers the data from all the users and transfers it to the central server periodically, where clinicians can classify the user's health status. One of the major issues in these remote health monitoring systems is the continuous data transmission, which leads to the hyper connectivity scenario [4][5]. In [6], intelligent indoor positioning algorithm that fuses a Pedestrian Dead Reckoning (PDR) system and an Received Signal Strength (RSS) based Wi-Fi positioning system is discussed. Wireless Body Area Networks (WBAN) applications like intra-space suit radio propagation channel in various frequency bands including 2.4 GHz is discussed in [7]. In remote health care monitoring application we cannot make use of the available bandwidth effectively, if we use the traditional mode of transmitting the data continuously. It reduces the node life time, even leads to loss of data due to delay and buffer overloading, which is not acceptable particularly in the health care applications.

Other issue, the Internet of Things (IoT) architectures face is the anywhere or ubiquitous connectivity, especially in WBAN applications where the patient is needed to be under constant supervision of the clinicians for proactive diagnosis. Bluetooth, ZigBee and Wi-Fi are the primary suite of high level communications used in WBANs. WBAN systems would have to ensure seamless data transfer across standards such as Bluetooth LE, ZigBee and Wi-Fi etc. to promote information exchange, plug and play device interaction. ZigBee and Bluetooth LE assists in a low energy consumption with low data rate but offers very low range compared to Wi-Fi. Being a mobile user under monitoring, the chances of user loosing connectivity by crossing the range is very high which makes the delivery of proactive diagnosis a difficult aspect.

In this paper we propose a system architecture for multi parametric remote health monitoring which can address the issues discussed above. The rest of the paper is structured as follows. Section II discusses the holistic view of proposed low power ubiquitously connected system architecture and the internal functional units. In section III, we discussed the environment and user mobility modelling. Section IV includes the performance analysis of the proposed system architecture

and the FPGA based hardware prototype developed in IIT Hyderabad. It also discusses the hardware complexity analysis of the proposed seamless hand-off controller and adaptive rule engine. Section V concludes the paper by discussing the future scope of the work.

II. Holistic View of Proposed Low Power Ubiquitously Connected System Architecture

The holistic view of the system architecture is shown in Fig. 1. The signal acquisition acquires the multi parametric medical data such as Electro Cardiogram (ECG), body temperature, glucose levels, heart beat etc. from different sensors using various signal processing techniques. Better proactive diagnosis can be given only if the data collected from the patient is classified properly. This intelligent classification can be achieved by extracting important features (such as PR, QRS and QT intervals from ECG signal and body temperature from temperature data) from the collected medical data, from which we can discover the abnormalities in the patient. This process of collecting features from the patients physiological data is known as feature extraction. The features extracted are then supplied to adaptive rule engine, which then classifies the data into abnormal or normal. The adaptive rule engine after classifying the data decides whether the data has to be transmitted or not based on an automated decision making algorithm. If the adaptive rule engine decides to transmit the data, the seamless hand-off controller chooses an appropriate radio from the available multiple on-chip radios depending on the range vicinity and radio energy consumption. As a proof of concept, we are considering the system monitoring ECG signal from the patient with ZigBee and Wi-Fi as the on-chip multiple radios available but no limitation on number of radios.

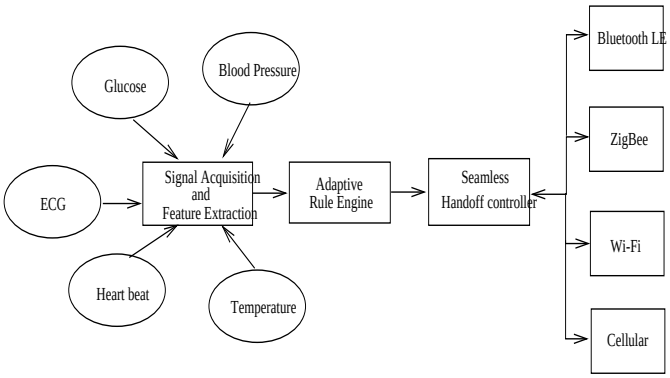

Fig. 1: System architecture of low power ubiquitously connected remote health monitoring system with smart transmission mechanism

Many architectures for the ECG signal acquisition system have been developed in the past [8], [9] & [10]. For the analysis of performance Lead I ECG data is considered. The data acquisition system developed at IIT Hyderabad has an upper cutoff frequency of 0.5 Hz and a lower cutoff frequency of 120 Hz with a sampling rate of 1000 Hz. Feature extraction plays an important role in automating the remote health monitoring. Identification of points such as P, Q, R, S and T shown in Fig. 2

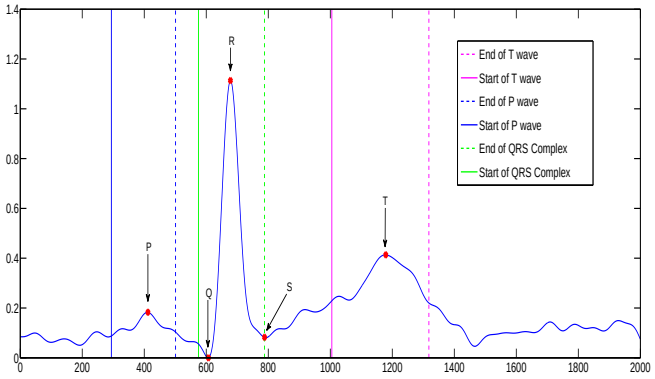

Fig. 2: PQRST complex from the collected Lead I Digital ECG data

from the Lead I ECG signal plays prominent role in calculating the required features and helps in classifying the patient. For a detailed description of several feature extraction algorithms available, kindly refer to [11], [12] & [13]. In following sub sections the functionality of adaptive rule engine and seamless hand-off controller are discussed in detail.

A. Adaptive rule engine based smart transmission mechanism

Using the adaptive rule engine mechanism the transmission can be made smart which reduces the amount of data to be transmitted thereby reducing the energy consumption. Performance analysis of the adaptive rule engine based smart transmission system has been analyzed in [9]. In [9], the authors have considered remote ECG monitoring system with ZigBee communication facility. In this paper, we extend the analysis to multiple on-chip radios scenario, where the selection of radios is done intelligently. The inputs to the adaptive rule engine are the features extracted from the collected medical data. In ECG signal, these features primarily include PR interval, QRS interval and QT interval.

The adaptive rule engine makes use of two thresholds, *soft threshold* and *hard threshold* to classify the data. Considering ECG monitoring as the target application, the key features that doctors use to classify the data are listed in the TABLE I. The values listed in the TABLE I are normal ranges of the ECG signal for a healthy patient [14] and are used as the *hard threshold*, which is the bounding limit of perfectly healthy ECG data. The *soft threshold* is an internal variable, which is initialized to *hard threshold* and whenever the sensed value exceeds the current *soft threshold*, the *soft threshold* is reset to the sensed value. In the first iteration, the parameters observed from the data are compared with the *hard threshold* values. If any of the parameter exceeds, it is classified as an abnormal data and it is again compared with the *soft threshold*. If the parameter values exceed the *soft threshold* parameters, the parameters in the *soft threshold* corresponding to the exceeded parameters of the collected data are reassigned with the parameters acquired from the user and transmits the collected data. In the second case, where the parameters of collected data do not exceed *soft threshold*, will only enable

the abnormality indicator resulting in no transmission of data but stores the data on the on board storage. Using this smart transmission, the amount of data to be transmitted can be reduced drastically without losing the accuracy on patient condition and without losing any data.

Case	Parameter	Normal Threshold
1	PR interval	0.12 - 0.20 Sec
2	QRS interval	$\leq$ 0.12 Sec
3	QT interval	$\leq$ 0.42 Sec

TABLE I: Threshold values of the intervals

TABLE II, depicts the flow of generic adaptive rule engine with ECG monitoring for 3 iterations. The system is assumed to continuously collect sets (1 set = 30 seconds duration) of ECG data. Observed data is the average of features collected within a single set of data. In iteration 1, the observed value of PR interval is 0.21 which exceeds both the *hard threshold* and *soft threshold*. Hence the data is transmitted and *soft threshold* is adjusted accordingly. In iteration 2, the observed value of PR interval exceeds *hard threshold* but does not exceed *soft threshold*. Hence the data is not transmitted but stored onto on board storage thereby guaranteeing no loss of data. The rest of the iterations work in similar fashion. After a particular number of iterations (10 in this case), *soft threshold* is again reset to *Hard threshold*.

B. Proposed intelligent seamless hand-off mechanism

Seamless hand-off mechanism controls the hand-off (switching and selecting) between multiple radios depending on the physical location of user predicted using Received Signal Strength Indication (RSSI). The ubiquitous connectivity of the user to the network is of primary importance, which can be achieved by the help of seamless hand-off mechanism controlled by the seamless hand-off controller (SHC). Main purpose of the SHC is to select appropriate radio depending on the range vicinity and radio energy consumption. The SHC selects the radio which consumes less energy and also has connectivity among the available on-chip radios. In this paper we considered ZigBee and Wi-Fi as the available on-chip radios for SHC, but equally adaptable to any number of radios such as Bluetooth LE and cellular networks.

At the beginning, the transmission always starts with the user ZigBee scanning for a network, if it finds one it joins and starts communicating with the gateway else SHC decides to scan for any available Wi-Fi networks in the vicinity. If none of the radios are available, the user starts using cellular facility. The communication initialization flow is shown in Fig. 3. In the following sections each of the scenarios encountered by the SHC is described in detail.

C. SHC scenario 1 (ZigBee available during communication initialization)

In scenario 1, user starts the communication with the gateway using ZigBee. Whenever the user transmits the packet containing the payload, gateway upon receiving the packet

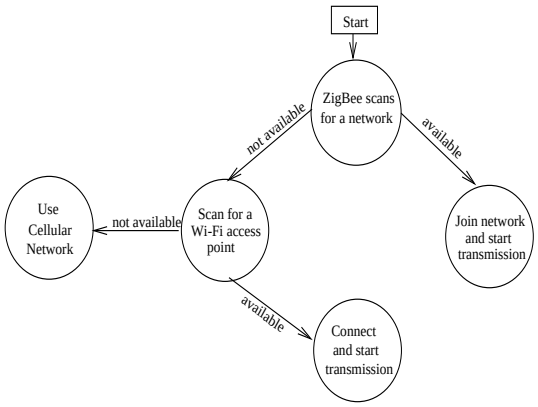

Fig. 3: Initialization flow for communication by the user

calculates the Received Signal Strength from RSSI. RSSI indicates the power in the received signal and a procedure to measure RSSI has been depicted in [15]. Based on the RSSI the gateway suggests the user to make a hand-off if necessary. Fig. 5 shows the complete functionality of SHC in scenario 1. For every packet received by the gateway, it acknowledges the user with a specific packet containing the information relating to the hand-off and the retransmission. The structure of the acknowledgement packet is shown in Fig. 6. The retransmit indicator and hand-off indicator bits contain the information pertaining to re-transmission of the last sent packet and the hand-off respectively. Based on the transmission quality, acknowledgement packets are classified into four types. The description of all the four types of acknowledgments are furnished in TABLE VI. If the RSSI value of the received packet falls below a particular threshold then the gateway suggests the user for a hand-off by sending a type II or type IV acknowledgement depending on whether the received packet is error free or not. The complete flow of the SHC on the gateway for generation of acknowledgement is shown in Fig. 4.

Considering a healthy patient as the end user, the duty cycle of the transmitter will be very low with the smart transmission achieved using the proposed adaptive rule engine. In such cases the user may come out of the ZigBee network vicinity and when the user attempts a transmission, it results in a loss. To prevent such cases every time the user is in a sleep mode, the user performs connection status mechanism with the gateway periodically at an interval of T seconds, where the user initially scans for beacon messages from the gateway. If there are any beacon messages from the gateway immediately user transmits a connection status query frame which consists of source address, node id and destination address. In turn the user expects a connection response which has the acknowledgement frame shown in Fig. 6 embedded into it. Upon using this kind of connection status mechanism, the gateway can suggest the user with hand-off if the node is about to go out of the vicinity of the ZigBee gateway thereby preventing the information losses. After crossing the range of ZigBee and started the communication using Wi-Fi, there are possibilities where the user comes back into the

Parameter	Initial values		Iteration 1			Iteration 2			Iteration 3		
	Hard threshold (Sec)	Soft threshold (Sec)	Observed value	Hard threshold (Sec)	Soft threshold (Sec)	Observed value	Hard threshold (Sec)	Soft threshold (Sec)	Observed value	Hard threshold (Sec)	Soft threshold (Sec)
PR Interval	0.12 - 0.20	0.12 - 0.20	0.21	0.12 - 0.20	0.12 - 0.21	0.21	0.12 - 0.20	0.12 - 0.21	0.22	0.12 - 0.20	0.12 - 0.22
QRS Interval	0.12	0.12	0.11	0.12	0.12	0.12	0.12	0.12	0.11	0.12	0.12
QT Interval	0.42	0.42	0.41	0.42	0.42	0.40	0.41	0.41	0.42	0.41	0.42
			Abnormality = Yes			Abnormality = Yes			Abnormality = Yes		
			Data transmitted			Data not transmitted, Stored to on board memory			Data transmitted		

TABLE II: Flow of generic adaptive rule engine for 3 iterations in ECG monoitoring

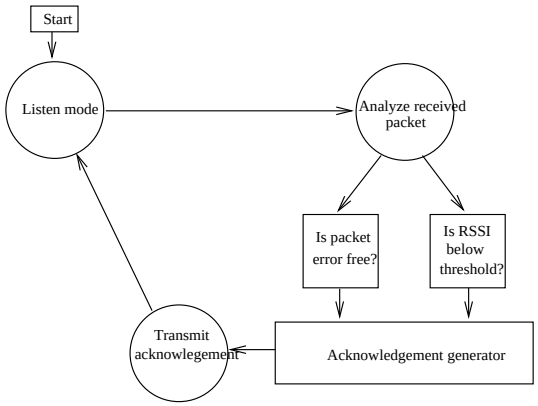

Fig. 4: Acknowledgment generation by SHC on the gateway

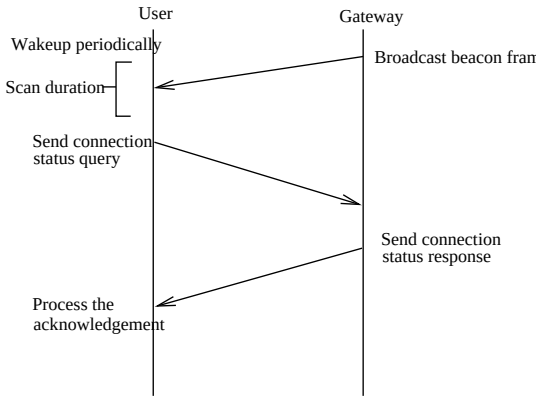

Fig. 7: Flow of connection status process in scenario 2

Fig. 5: Process of SHC in scenario 1 on both user and gateway

vicinity of the ZigBee. In such cases the same connection status mechanism can be used for making hand-off back to ZigBee. As the Wi-Fi is in transmitting state and ZigBee is in sleep mode, ZigBee on the user device wake up at the periodic intervals and performs the connection status procedure. ZigBee on user node, while performing the connection status process it will have to co exist along with the Wi-Fi which operates in the same frequency band of 2.4 GHz which may result in co-interference between the radios. In [16], [17] & [18], the performance of different technologies operating at 2.4 GHz frequency during their coexistence have been analyzed. The analysis shows that ZigBee has less effect on the Wi-Fi transmission.

Type	(Retransmit, Hand-off) indicator	Description
I	(0,0)	No retransmit, no hand-off required
II	(0,1)	No retransmit, make a hand-off
III	(1,0)	Retransmit, no hand-off required
IV	(1,1)	Both retransmit and hand-off required

TABLE III: Types of acknowledgements

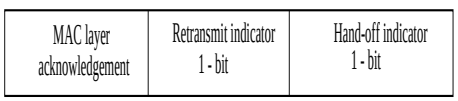

Fig. 6: Structure of the acknowledgement

D. SHC scenario 2 (ZigBee is not available during communication initialization, but Wi-Fi is available)

In scenario 2, user starts the data transfer using Wi-Fi. While the user is transmitting the data using Wi-Fi, user also performs the connection status mechanism using ZigBee as discussed in scenario 1 and proper hand-off is made accordingly. The flow of the connection status process is shown in Fig. 7.

In cases where the user starts moving out of the range of Wi-Fi, the RSSI values fall gradually. At a point, the RSSI value falls to a minimum threshold value where a hand-off is necessary from Wi-Fi to cellular network. In this case the user node immediately establishes connection with the local base station in case of 2G or remote radio heads in case of LTE network.

E. SHC scenario 3 (Wi-Fi and ZigBee are not available)

In scenario 3, the user position is assumed to be out of the range of both the ZigBee and Wi-Fi. In such cases, user begins his communication initialization process with ZigBee scanning for any available networks with which the user can associate. Since the node is not in the vicinity of the ZigBee network, the user switches to Wi-Fi and scans for any available access points. Finally as the user does not find any access point, he uses cellular network as the communication mechanism. The communication initialization in scenario 3 is shown in Fig. 8.

After starting the communication using cellular network, the user may come into the vicinity of ZigBee or Wi-Fi where the user will have to prefer communicating using one of them. The user continuously performs connection status for both ZigBee and Wi-Fi periodically. The connection status process in scenario 3 is shown in Fig. 9. The user periodically performs

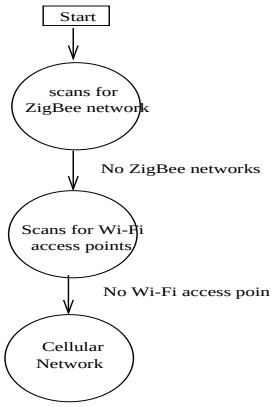

Fig. 8: Communication initialization in scenario 3

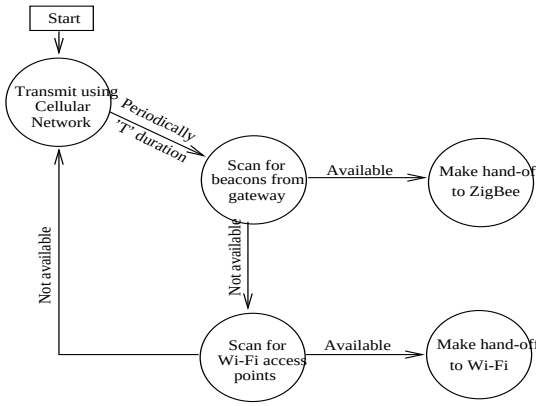

Fig. 9: Connection status process in scenario 3

communication status process for ZigBee and Wi-Fi. If any of the two modes of communication is available, user then makes a proper hand-off based on the hand-off indicator. If both of them are available user prefers ZigBee to Wi-Fi.

III. Environment and user mobility modeling

For analyzing the performance of the on-chip adaptive rule engine based smart transmission technique with on-chip seamless hand-off mechanism based multiple radio communication system, twenty users, having both the ZigBee and Wi-Fi based communication facilities are considered. The mobility of the users have been modeled using '*random way point mobility pattern*' and the path loss estimation is made using the *'Attenuation Factor model'*. The users are assumed to be moving randomly in a room of dimensions 100m X 100m. The complete flow involved in the environment and user mobility modeling is shown in Fig. 10 and is described briefly in following sections.

A. Random way point mobility pattern (RWP)

The mobility of the 20 users, has been modeled using Random Waypoint Mobility (RWP) pattern [19]. All the mobile nodes are distributed randomly around the entire area. The parameter *pause time* determines the period of time the user stays at one location and as soon as the pause time expires, the

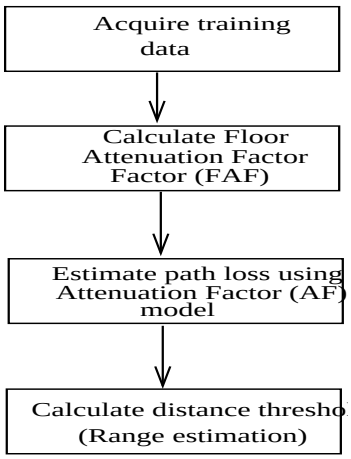

Fig. 10: Flow involved in environment and user mobility modeling

user selects a random destination around the area and starts moving at a uniform speed which is uniformly chosen from *max speed* and *min speed*. The mobility pattern of the 20 users is shown in Fig. 11 and the parameters of the RWP mobility pattern are depicted in TABLE IV. The pause interval is uniformly chosen from 0 to 1 seconds and the minimum and maximum velocities of the mobile node considered are 0.1 and 0.3 m/s, which is a valid assumption in mobile health care monitoring applications.

Parameter	Value
Area	100 X 100 Sq.mt.
Minimum speed	0.1 m/s
Maximum speed	0.3 m/s
Pause interval	[0 1]

TABLE IV: RWP mobility pattern parameters

In Fig. 11, the position of the gateway is indicated using a red square at the center. The boundaries of the mobility for twenty users has been indicated in different colors. The red dashed circle indicates the estimated range of ZigBee coverage using the '*Attenuation Factor Model*' [20], [21] & [22]. The rest of the performance analysis is made using the mobility pattern shown in Fig. 11.

Observing Fig. 11, we can infer that users 13 and 1 (indicated in red and blue path) lie ,most of the time within the range of ZigBee coverage and uses Wi-Fi less frequently when compared to other users. The mobility of all the users for the entire one hour duration is shown in Fig. 12, where the x-axis indicate the time in seconds and y-axis indicates the distance of the user from the gateway. One can observe the times at which users are crossing hand-off boundary.

B. Range estimation for ZigBee

The range of the ZigBee coverage should be estimated for deciding the hand-off threshold distance. In general the receiver sensitivity of ZigBee is -95 dBm, beyond which the error rate increases and quality of the transmission will be

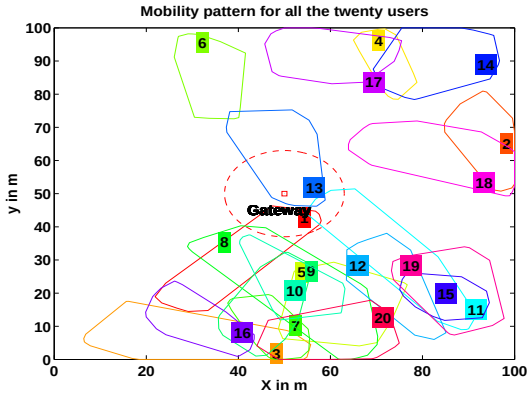

Fig. 11: Mobility pattern for all the 20 users

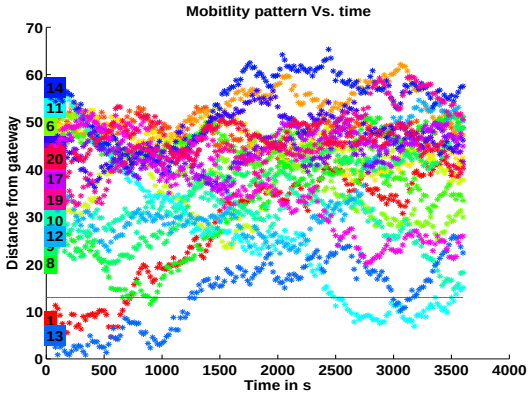

Fig. 12: Coverage of all 20 users with time

poor. For making a hand-off, a safer threshold of -85 dBm is considered. The hand-off threshold distance of the ZigBee is equal to the distance at which the received power equals the hand-off threshold power and is obtained using the Attenuation Factor model and the RSSI values obtained from the training data.

1) Attenuation factor model: Many indoor path loss models have been proposed such as Log-distance model, Ericsson multiple breakpoint model and Attenuation factor model (AF) [22] etc. From the AF model, the path loss at a distance *d* in indoor scenarios, can be found using the equation (1).

$$\begin{aligned} \bar{PL}(d)[dB] &= \bar{PL}(d_0)[dB] + 10\eta \log(\frac{d}{d_0}) + FAF[dB] \\ \bar{PL}(d)[dBm] &= \bar{PL}(d)[dB] + 30 \end{aligned} \quad (1)$$

In equation (1), the $\bar{PL}(d)[dB]$ is the path loss at a distance d in dB, $\bar{PL}(d_0)[dB]$ is the path loss at a distance d_0 and FAF is the floor attenuation factor in dB. η represents the path loss exponent value for the same floor. The equation (1) can be rewritten as shown in (2)

$$\bar{PL}(d)[dBm] = \bar{PL}(d_0)[dBm] + 10\eta \log(\frac{d}{d_0}) + FAF[dB] \quad (2)$$

For a better estimation of the path loss, a better estimate of the parameters η and FAF are required. The standard values for the two parameters in different scenarios are given in [22]. These parameters cannot be considered as a perfect estimation, since they are scenario dependent and the parameters are

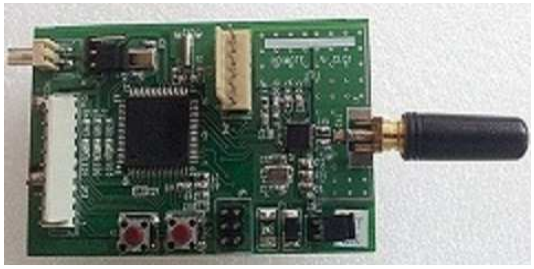

Fig. 13: IITH mote developed in IIT Hyderabad

affected by various environmental changes, such as occupancy in the room, partitions in the room and user movements etc. Hence the parameter FAF is found out using the RSSI values obtained during the training phase. The FAF calculated from different trials is found out to follow the normal distribution.

2) Training phase: For the training phase, the data collected using the in house developed ZigBee node at IIT Hyderabad namely 'IITH mote' [23] shown in Fig. 13 is used. During the training phase, the RSSI which gives the received signal strength at various distances is collected. Fig. 14 shows the average RSSI over hundred trials measured at different distances. The received signal strength decreases as the distance from the gateway increases. From the RSSI values collected at different distances, the FAF is estimated using the equation (2). For the FAF estimation d_0 is estimated to be 1m, which reduces the equation (1) to the form shown below.

$$\begin{aligned} \bar{PL}(d)[dBm] &= \bar{PL}(d_0)[dBm] + 10\eta \log(d) + FAF[dB] \\ d_0 &= 1m \end{aligned} \quad (3)$$

Now the path loss at a distance of 1m can be found using the equation 4, where $\bar{PL}(1m)[dBm]$ indicates the path loss at a distance of 1m and P_t, P_r are the transmitted and received power at a distance of 1m respectively. The transmit power used is 3 dBm and the received power at 1m distance can be calculated from Fig. 14, which is -48 dBm approximately for an η of 2.68. Based on the RSSI values collected at different distances from the gateway, the FAF is estimated and the density function of FAF extracted from the collected data over different trials is shown in Fig. 15. The probability density function is evaluated over hundred trials at different distances and is averaged over different distances. It is found out that the average probability density function resembles the probability density function of a normal random variable.

$$\bar{PL}(1m)[dBm] = P_t - P_r(1m) \quad (4)$$

From the average probability density function of FAF calculated from training phase the mean of the FAF is calculated to be 8.684 dB and standard deviation is calculated to be 2.3616. For the rest of the analysis in the paper the FAF is assumed to be a normal random variable with mean 8.684 dB and standard deviation of 2.3616. Upon averaging the path losses over a number of trials, the path loss obtained is shown in Fig. 16. From Fig. 16, we can observe that at a distance of 13 m, the path loss is approximately 88 dBm, which is the hand-

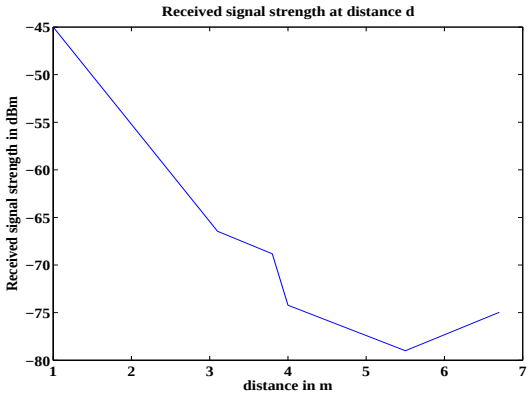

Fig. 14: Average received signal strength in dBm at different distances

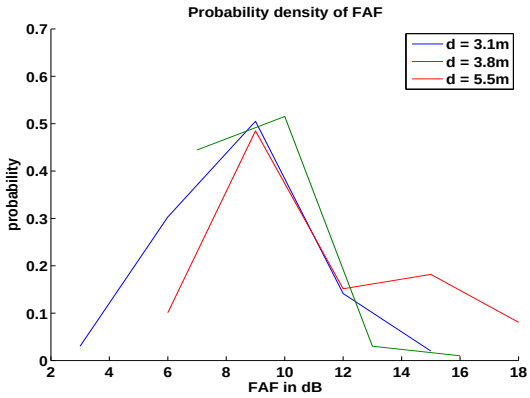

Fig. 15: Probability density function of FAF extracted from training phase

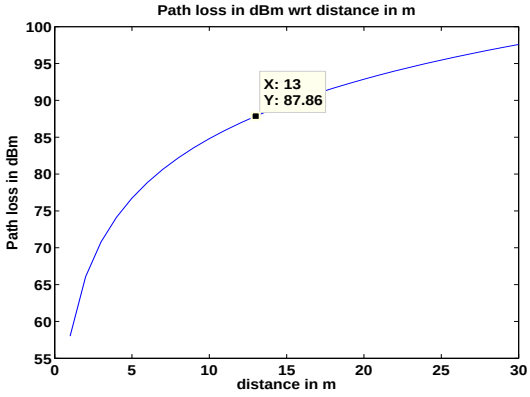

Fig. 16: Average path loss estimation at distance d

off threshold.Thus theoretical analysis using the training data gives 13 m as the hand-off threshold distance.

IV. Performance Analysis

In this section we analyse the performance of the proposed system architecture for low power ubiquitously connected remote health monitoring system with smart transmission mechanism and hardware prototype used for field trials. The performance metrics used for the performance evaluation are energy consumption, network node lifetime and data losses.

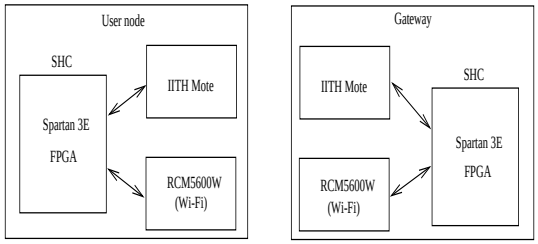

Fig. 17: Architecture of the hardware prototype

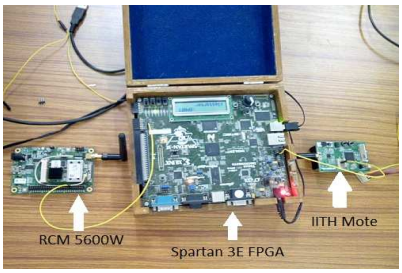

Fig. 18: Hardware prototype developed in IIT Hyderabad

The specifications of the ZigBee and Wi-Fi used are shown in TABLE V.

Parameter	Value for ZigBee	Value for Wi-Fi
Current consumption in transmit state	40 mA	625 mA
Current consumption in sleep state	3.5 μA	10 μA
Time for transition from sleep to transmit state	1.2 mSec	2.2 mSec
Time for transition from transmit to sleep state	1 mSec	2 mSec
Transmit power	3 dBm	17 dBm
Receiver sensitivity	-90 dBm	-90 dBm
Range (indoor)	30m (approx.)	100 m (approx.)

TABLE V: Specifications of ZigBee and Wi-Fi devices used

A. Architecture of FPGA based hardware prototype

A FPGA based hardware prototype for the proposed adaptive rule engine based smart transmission with seamless hand-off mechanism among multiple radio communication system architecture is developed in IIT Hyderabad. The architecture of the prototype is shown in Fig. 17 and Fig. 18 shows the Spartan 3E FPGA based hardware prototype developed in IIT Hyderabad. For the prototype development, IITH Mote is used as a ZigBee device and RCM5600W [24] is used as the Wi-Fi device. Spartan 3E FPGA is used to implement the adaptive rule engine based transmission system and seamless hand-off controller. Using the prototype developed, the hand-off boundary in a room of dimensions 9.8m X 7m is found. The environment in the room is similar to an office scenario having soft and hard partitions, with people moving randomly. The hand-off border is calculated as an average over 20 trials. Fig. 19 shows the hand-off border, RSSI values at different distances and the partitions in the room.

In Fig. 19, the dashed line indicates the hand-off border. The area behind the soft partition comes out of the range of ZigBee coverage, due to the presence of many obstacles. The average range of ZigBee coverage is approximately 12.6 m. At a distance of 6.7 m, the received signal strength by the user node is observed to be -79 dBm which shows a very good correlation between the theoretical path loss derived shown in

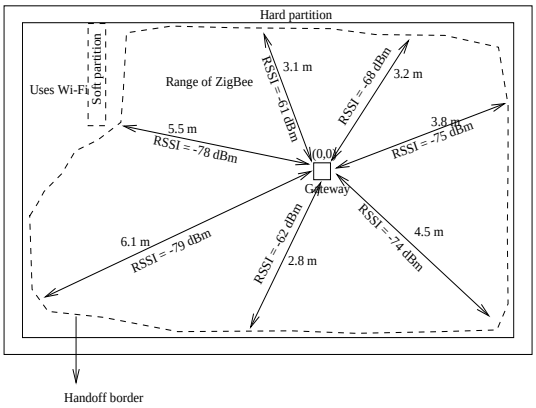

Fig. 19: Handoff border achieved from the field trials

Fig. 16 and path losses collected from the experimental field trials.

B. Energy Consumption and Life Time of Network Node

Analytic models for energy consumption of the sensor nodes are discussed in [9], [25] & [26]. For the analysis, they have considered energy consumed by the processor, transceiver and sensors. In this paper, we considered only the energy consumed by the transmitter with the seamless handoff controller controlling the radios, as the other parameters remain constant for the analysis. For the modeling of energy consumption, the transmitter is assumed to operate only in two states, on and off state. The energy consumed by the transmitter can be calculated as the sum of energy consumed in a particular state (on or off) and energy consumed for the state transitions.

$$E_{cons} = E_{state} + E_{trans} \tag{5}$$

$$E_{state} = \sum_{i} \frac{P_{TX} L_i}{R} + P_{Off} T_{Off} \tag{6}$$

$$E_{trans} = j \times P_{on-off} T_{on-off} + k \times P_{off-on} T_{off-on} \tag{7}$$

The E_{cons} in equation (5) shows the over all energy consumption by the transmitter. It is the sum of energy consumed in the two states (on, off) E_{state} and energy consumed for state transitions (on to off, off to on) E_{trans} by the transmitter. The P_{TX} and P_{off} indicates the power consumption in transmitting and off state respectively. T_{off} is the total time the transmitter spent in the off state. L_i and R indicates the data length to be transmitted (headers + payload) and maximum input data rate supported by the corresponding radio respectively. i indicates the packet number. P_{on-off} and P_{off-on} indicates the power consumed during the state transition from on to off and off to on respectively and the corresponding transition times are T_{on-off} and T_{off-on}. j and k indicates the number of transitions from on to off state and off to on states by the radio respectively.

In analyzing the energy consumption for all the three scenarios, we have to consider the packet structures for both the ZigBee and Wi-Fi. The energy consumed is directly proportional to the packet length. The ZigBee packet has a maximum size of 133 bytes and carry 104 bytes of payload at the maximum [27]. The rest of the 29 bytes accounts for the header fields. Whereas Wi-Fi has a maximum payload support of 2312 bytes in a single packet [28], but in TCP it is limited by maximum transmission unit (MTU) which is 1500 bytes [29]. Here the transmission using TCP has been assumed, and the maximum payload that can be transmitted in a single packet is considered to be 1500 bytes. A single packet in Wi-Fi has a size of 1524 bytes, where 24 bytes account for header fields. The number of packets required to be transmitted can be calculated using the equation (8) and total length of data to be transmitted is given by equation (9).

$$N = \frac{L_{data}}{L_{max\ payload}} \tag{8}$$

$$L_i = N \times L_{packet} \tag{9}$$

In equation (8), N refers to the number of packets, L_{data} and $L_{max\ payload}$ are length of data and length of maximum payload per packet in bytes. In equation (9), L_i indicates the data length to be transmitted by the radio in bytes.

The energy consumption is analysed in two scenarios, constant burst transmission and the adaptive rule engine based smart transmission.

1) Constant burst transmission with seamless handoff controller: In this scenario the user constantly transmits the data at a data rate of 250 Kbps (maximum data rate supported by ZigBee) and no intelligent transmission mechanism is used in this scenario. The user mobility shown in Fig. 11 is considered for the energy consumption analysis. Fig. 20 shows the energy consumption for all the twenty users when transmitting continuously at a constant bit rate. From the Fig. 20 we can see that user 13 consumes very less energy of 6.09 J compared to users 2, 3 & 4 consuming 9.77 J due to the fact that user 13 spends most of the time within the vicinity of the ZigBee. The lifetime of the individual nodes is shown in Fig. 21, where the user 13 has maximum life time of 0.511 years.

2) Adaptive rule engine based smart transmission with seamless handoff controller: In the previous scenario, we used a continuous burst transmission technique which consumes more power and also increases amount of traffic. Energy consumption by the twenty users in the adaptive rule engine based smart transmission with seamless handoff mechanism is shown in Fig. 22. From Fig. 22, we can see that user 13 consumes very less energy approximately 2.56 J compared to user 2, who consumed approximately 4.86 J. When compared to the continuous transmission scenario, the energy consumption in adaptive rule engine based smart transmission scenario is very less. On an average of 20 users the energy consumed in the constant burst transmission scenario is 9.3389 J, which is very high compared to 4.6329 J in adaptive rule engine based smart transmission scenario. This shows that there is a 50.39% of reduction in energy consumption when using the adaptive rule engine based smart transmission when compared to the constant burst transmission scenario. The lifetime of the

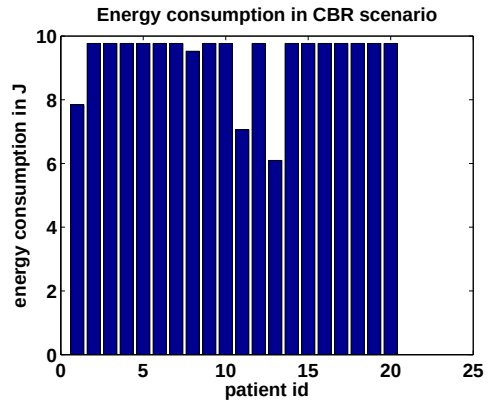

Fig. 20: Energy consumed with continuous transission for all the 20 users

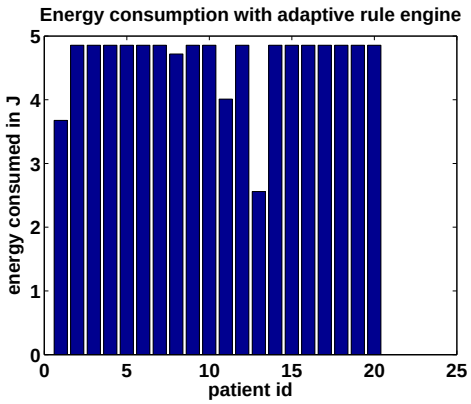

Fig. 22: Energy consumption in adaptive rule engine based smart transmission scenario

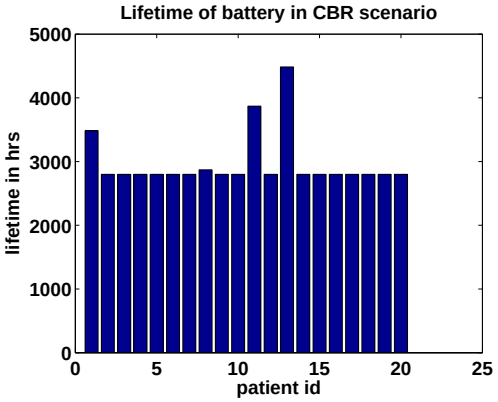

Fig. 21: Estimated battery lifetime in continuous transmission scenario

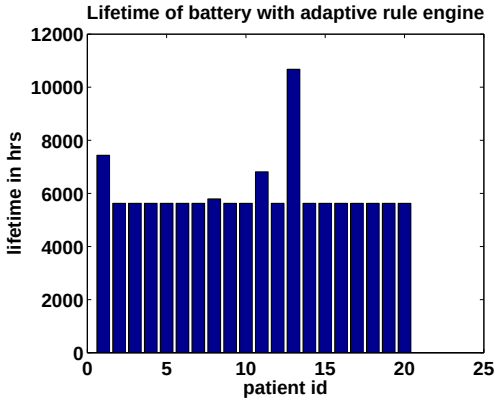

Fig. 23: Estimated battery lifetime in adaptive rule engine based smart transmission scenario

individual nodes is shown in Fig. 23, where the user 13 has maximum life time of 1.22 years when using the adaptive rule engine based smart transmission compared to 0.511 years in constant burst transmission scenario.

Fig. 24 plots the duty cycle of a node versus time in seconds. Adaptive rule engine is operated on the 3 sets of data (90 seconds of data) and it can be observed that the transmitter of node is only awake for first set out of 3 sets, thereby reducing the duty cycle of transmitter by 66% compared to constant burst scenario mechanism where the transmitter is in on state always. On an average over 20 patients, the duty cycle of the transmitter is observed to be 48.99 %, which leads to a significant saving in energy. Fig. 25, plots data loss for every patient when using only ZigBee for communication and in the presence of multiple on-chip radios. One can clearly observe the data losses are high upon using only ZigBee radio. Hence the use of multiple on-chip radios can greatly aid in loss less transmission of data with less delay and very less energy consumption.

C. Hardware complexity analysis

1) Seamless hand-off controller: Fig. 26 shows the hardware architecture for seamless hand-off controller. The hardware complexity depends primarily on 16 bit comparator. It compares received signal RSSI value with the predefined threshold value, which enables the suitable radio for transmission. The threshold value used in this study is -85 dBm. Table VI and Table VII shows the total number of logic gates and Complementary Metal Oxide Semiconductor (CMOS) transistors required to implement the seamless hand-off controller. From the analysis made it shows that the seamless handoff controller is very low complex that it requires only 608 CMOS transistors for implementation.

Type of logic gate	16 bit comparator
AND	64
OR	16
NOR	16
NOT	32

TABLE VI: Hardware complexity of Seamless hand-off algorithm in number of logic gates

Type of logic gate	No.of CMOS Transistors
AND	384
OR	96
NOR	64
NOT	64

TABLE VII: Hardware complexity of Seamless hand-off algorithm in number of CMOS Transistors

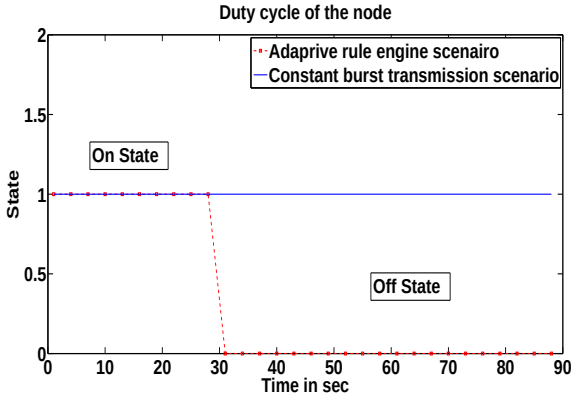

Fig. 24: Duty cycle of the node in adaptive rule engine based smart transmission scenario

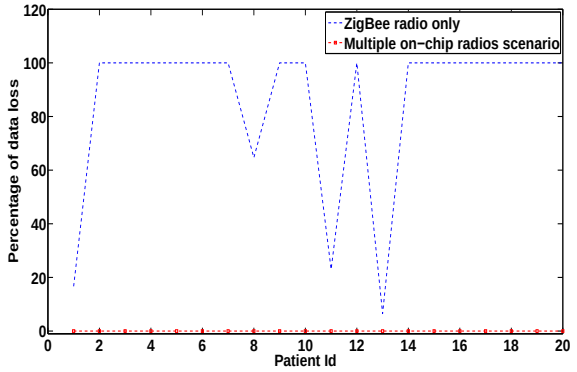

Fig. 25: Data loss per patient in adaptive rule engine based smart transmission scenario with single radio and multiple radios

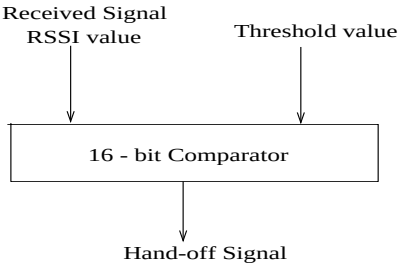

Fig. 26: Hardware architecture of the seamless hand-off controller

D. Adaptive rule engine

The hardware architecture of adaptive rule engine is as shown in Fig. 27, which requires two 16 bit comparators, two 3 bit adders, one 3 bit comparator and one 16 bit subtractor. The 16 bit subtractor serially calculates the PR, QRS and QT data intervals of ECG signal from their respective start and end points from the input data. The data intervals are then compared with corresponding hard threshold values using a 16 bit comparator and a decision is made $i.e.$ normal or abnormal. Based on the decision made at hard threshold, if the data is found to be abnormal second 16 bit comparator compares with the soft threshold values. If it does not exceed

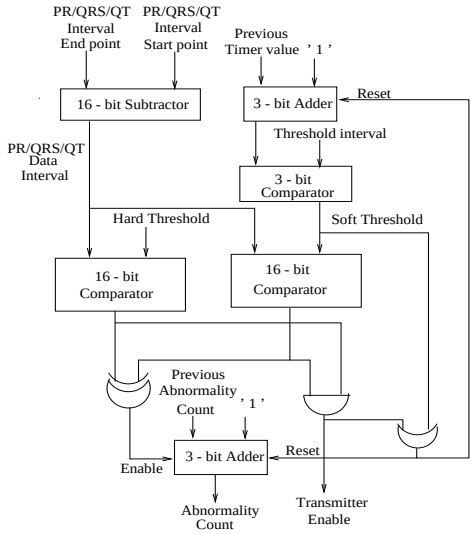

Fig. 27: Hardware architecture of the Adaptive Rule Engine

soft threshold, abnormality count is increased using a 3 bit adder and timer is incremented using second 3 bit adder, if data intervals exceed soft threshold value the data is transmitted using control section and resets abnormality count and timer. The output of 3 bit comparator is also used to reset both soft threshold and timer values when timer value exceeds the predefined threshold value. Table VIII and Table IX shows the total number of logic gates and CMOS transistors required to implement the proposed adaptive rule engine. From the analysis made it shows that the seamless handoff controller is very low complex that it requires only 1588 CMOS transistors for implementation.

Type of logic gate	16 bit subtractor	Two 16 bit comparators	Two 3 bit adders	3 bit comparator	Total gates count
AND	31	64	4	12	112
OR	15	32	2	3	53
XOR	48	0	4	0	53
NOR	0	32	0	3	35
NOT	0	64	0	6	70

TABLE VIII: Hardware complexity of Adaptive Rule Engine in number of logic gates

Type of logic gate	No.of CMOS Transistors
AND	672
OR	318
XOR	318
NOR	140
NOT	140

TABLE IX: Hardware complexity of Adaptive Rule Engine in number of CMOS Transistors

V. Conclusion

In this paper, we proposed a system architecture of low power ubiquitously connected remote health monitoring system with smart transmission mechanism. We proposed a seamless hand-off mechanism to intelligently select the radio among multiple on-chip radios. Three different scenarios of seamless hand-off controller were investigated and the performance of the system is evaluated. For the performance evaluation, ECG data of 20 patients with different age groups were

considered. The radio range obtained from the experimental results for the ZigBee matches very well with the threshold range estimated using Attenuation Factor model. The proposed seamless hand-off controller (SHC) achieves a 50.39% of reduction in energy consumption and 51.01 % of reduction in duty cycle of transmitter. Irrespective of the user mobility, the proposed architecture guaranteed loss less transmission of data which is an important aspect in IOT enabled health monitoring systems. The proposed generic adaptive rule engine aids for significant reduction in network traffic when applied on ECG data thereby enhancing the network node lifetime. Performance analysis of the proposed seamless hand-off controller and adaptive rule engine shows that the architecture is very low complex requiring 2196 CMOS transistors.

Our future work is to explore the hardware multiplexing between the two radios and achieve a significant area reduction in the development of multiple radios based communication devices like an "IoT chipset". Envisaged IoT chipset will have features like adaptive rule engine based smart transmission technique to achieve low power and seamless hand-off controller (SHC) integrated for seamless hand-off between multiple on-chip radios to enable ubiquitous connectivity.

REFERENCES

[1] Rehunathan, D.; Bhatti, S.; Chandran, O.; Pan Hui, "vNurse: Using virtualisation on mobile phones for remote health monitoring," *e-Health Networking Applications and Services (Healthcom), 2011 13th IEEE International Conference on* , pp.82,85, 13-15 June 2011.

[2] Chowdhury, M.A.; McIver, W.; Light, J., "Data association in remote health monitoring systems," *Communications Magazine, IEEE* , vol.50, no.6, pp.144,149, June 2012.

[3] Priya, B.; Rajendran, S.; Bala, R.; Gobbi, R., "Remote wireless health monitoring systems," *Innovative Technologies in Intelligent Systems and Industrial Applications, 2009. CITISIA 2009* , vol., no., pp.383,388, 25-26 July 2009.

[4] Malik, Om., "Internet of things will have 24 billion devices by 2020", (GIGAOM), [online]. 2011, http://gigaom.com/2011/10/13/internet-of-things-will-have-24-billion-devices-by-2020/ (Accessed: 8 June 2014).

[5] The Mobile Economy 2014, GSMA, [online] 2014, http://www.gsmamobileeconomy.com/GSMA_ME_Report_2014_R2_WEB.pdf (Accessed: 8 June 2014).

[6] Chen, Lyu-Han; Wu, E.H-K.; Jin, Ming-Hui; Chen, Gen-Huey, "Intelligent Fusion of Wi-Fi and Inertial Sensor-Based Positioning Systems for Indoor Pedestrian Navigation," Sensors Journal, IEEE , vol.PP, no.99, pp.1,1 doi: 10.1109/JSEN.2014.2330573.

[7] Taj-Eldin, M.; Kuhn, W.; Hodges Fowles, A; Natarajan, B.; Peterson, G.; Alshetaiwi, M.; Ouyang, S.; Sanchez, G.; Monfort-Nelson, E., "Study of Wireless Propagation for Body Area Networks inside Space Suits," Sensors Journal, IEEE , vol.PP, no.99, pp.1,1 doi: 10.1109/JSEN.2014.2341178.

[8] S. Maheshwari, A. Acharyya, P. Rajalakshmi, P. E. Puddu and M. Schiariti (2013), Accurate and Reliable 3-Lead to 12-Lead ECG Reconstruction Methodology for Remote Health Monitoring Applications, *IEEE International Conference on e-Health Networking, Applications and Services (Healthcom, 2013)*, 9-12 October, 2013, Portugal, 2013.

[9] Kiran, M.P.R.S.; Rajalakshmi, P.; Bharadwaj, K.; Acharyya, A., "Adaptive rule engine based IoT enabled remote health care data acquisition and smart transmission system," *Internet of Things (WF-IoT), 2014 IEEE World Forum on* , vol., no., pp.253,258, 6-8 March 2014.

[10] Abdul Qayoon Bhat, Vineet kumar, Sunil Kumar, Design of ECG Data Acquisition System, *International Journal of Advanced Research in Computer Science and Software Engineering*, vol. 3, issue 4, April 2013.

[11] L. Y. Di Marco, Lorenzo Chiari, "A wavelet-based ECG delineation algorithm for 32-bit integer online processing," *Biomedical Engineering online*, vol. 10, no. 2, article 23, 2011.

[12] Mazomenos, E.B.; Biswas, D.; Acharyya, A.; Chen, T.; Maharatna, K.; Rosengarten, J.; Morgan, J.; Curzen, N., "A Low-Complexity ECG Feature Extraction Algorithm for Mobile Healthcare Applications," *Biomedical and Health Informatics, IEEE Journal of* , vol.17, no.2, pp.459,469, March 2013.

[13] Cuiwei Li; Chongxun Zheng; Changfeng Tai, "Detection of ECG characteristic points using wavelet transforms," *Biomedical Engineering, IEEE Transactions on* , vol.42, no.1, pp.21,28, Jan. 1995.

[14] Standard[online]. Available: www.meds.queensu.ca/central/modules/ECG/normal_ecg.html

[15] Benkic, Karl, et al. "Using RSSI value for distance estimation in wireless sensor networks based on ZigBee." *Systems, Signals and Image Processing, 2008. IWSSIP 2008. 15th International Conference on.*, 2008.

[16] Yue Tao; Xiang-Yang Li; Cheng Bo, "Performance of Coexisted WiFi and ZigBee Networks," *Distributed Computing Systems Workshops (ICDCSW), 2013 IEEE 33rd International Conference on*, pp.315,320, 8-11 July 2013.

[17] Garroppo, R.G.; Gazzarrini, L.; Giordano, S.; Tavanti, L., "Experimental assessment of the coexistence of Wi-Fi, ZigBee, and Bluetooth devices," *World of Wireless, Mobile and Multimedia Networks (WoWMoM), 2011 IEEE International Symposium on a*, pp.1,9, 20-24 June 2011.

[18] Shuaib, K.; Boulmalf, M.; Sallabi, F.; Lakas, A., "Co-existence of Zigbee and WLAN, A Performance Study," *Wireless Telecommunications Symposium, 2006. WTS '06*, pp.1,6, April 2006.

[19] Zola, Enrica; Barcelo-Arroyo, F., "Probability of hand-off for users moving with the Random Waypoint mobility model," Local Computer Networks (LCN), 2011 IEEE 36th Conference on , pp.187,190, 4-7 Oct. 2011.

[20] Phaiboon, S., "An empirically based path loss model for indoor wireless channels in laboratory building," *TENCON '02. Proceedings. 2002 IEEE Region 10 Conference on Computers, Communications, Control and Power Engineering* , vol.2, no., pp.1020,1023 vol.2, 28-31 Oct. 2002.

[21] Solahuddin, Y.F.; Mardeni, R., "Indoor empirical path loss prediction model for 2.4 GHz 802.11n network," *Control System, Computing and Engineering (ICCSCE), 2011 IEEE International Conference on*, pp.12,17, 25-27 Nov. 2011.

[22] T. S. Rappaport, *Wireless Communications: Principles and Practice.*, 2nd ed. Upper Saddle River,NJ:Prentice-Hall, 1996.

[23] P. Rajalakshmi, "IITH mote Wireless Sensor Communication Module", [online]. 2012, http://www.iith.ac.in/ raji/downloads/IITH-mote-webpage.pdf (Accessed: 8 June 2014).

[24] MiniCore RCM5600WC-Programmable Wi-Fi Core Module, [oline] 2010, http://www.digi.com/pdf/ds_rcm5600w.pdf (Accessed: 8 June 2014).

[25] H. Zhou, D. Luo, Y. Gao and D. Zuo, "Modeling of Node Energy Consumption for Wireless Sensor Networks," *Wireless Sensor Network*, Vol. 3 No. 1, 2011, pp. 18-23. doi: 10.4236/wsn.2011.31003.

[26] Ian F. Akyildiz, Mehmet Can Vuran, *Wireless Sensor Networks*, West Sussex: John-Wiley, 2010.

[27] IEEE Standard for Local and metropolitan area networks–Part 15.4: Low-Rate Wireless Personal Area Networks (LR-WPANs)," *IEEE Std 802.15.4-2011 (Revision of IEEE Std 802.15.4-2006)* , vol., no., pp.1,314, Sept. 5 2011 doi: 10.1109/IEEESTD.2011.6012487.

[28] IEEE Standard for Information technology–Telecommunications and information exchange between systems–Local and metropolitan area networks–Specific requirements Part 11: Wireless LAN Medium Access Control (MAC) and Physical Layer (PHY) Specifications Am," *IEEE Standard for Information technology–Telecommunications and information exchange between systems–Local and metropolitan area networks–Specific requirements Part 11: Wireless LAN Medium Access Control (MAC) and Physical Layer (PHY) Specifications Am* , vol., no., pp.,

[29] Kurose, James F. and Ross, Keith W., "Transport Layer" in *Computer Networking: A Top Down Approach*, 6th ed. NJ: Addison-Wesley, 2013, pp 185-302.